

No. 167 NARROW-BAND PHOTOMETRY OF THE GALILEAN SATELLITES

by WILLEM WAMSTEKER

May 30, 1972

ABSTRACT

Observations were made of the Galilean satellites in a narrow-band photometric system with a resolution of ~ 30 that covers the wavelength range from $0.3\text{--}1.1\mu$. The absolute scale of the system is determined from stellar model computations. It is concluded that 35 Leo, the main comparison star used, has an energy distribution similar to the sun. An attempt is made to interpret the albedo curves in terms of surface constituents.

1. Instrumentation

This paper is an attempt to use low-resolution spectrometry in the study of the surfaces of the Jovian satellites. This method was, among others, used successfully by McCord *et al.* (1970) on the asteroid Vesta, which led to the identification of pyroxene.

The Laboratory had acquired a set of 42 narrow-band interference filters from Infrared Industries, Thin Film Products Division, 62 Fourth Avenue, Waltham, Massachusetts. The bandwidth of the filters had been selected to represent a constant resolution of $\lambda/\Delta\lambda \sim 30$ over the full wavelength range

$0.3\text{--}1.1\mu$. The filters are mounted in three separate wheels each containing 14 filters, with the last filter repeated in the next set. The filter wheels were adapted to a single-channel photometer of the standard Johnson type (Johnson and Mitchell 1962).

An S-20 cathode was used for $0.30\text{--}0.72\mu$ and an S-1 for $0.72\text{--}1.1\mu$. The observations were made with the 61- and 40-inch telescopes of the Catalina Observatory, around the 1971 opposition of Jupiter. Owing to the low declination of Jupiter and the unfavorable summer observing conditions, the coverage is not as extensive as was intended. However all satellite data presented are an average of at least two observations on different nights.

Atmospheric extinction was allowed for by average extinction coefficients derived independently, checked on some nights by the observation of stars at small and large air masses. Allowance was also made for nights with high and low humidity within the well-known atmospheric water-vapor absorptions.

Table I gives the observations as "normalized" albedos, with the maximum put at unity. The values are ratios of the satellite intensities in terms of HR 4030 (35 Leo). Wavelength regions observed at different orbital phases of the satellites were adjusted to each other by means of the filters common to both data sets. The wavelengths in the first column of Table I are those midway between the 50 percent transmission points of the filters, assuming a flat radiation source.

2. Comparison Stars

A number of G2V-stars were observed to obtain sources with spectra similar to the sun. However, the average solar-type star is not identical to the sun, as shown by Code (1960). To acquire an independent estimate of the similarity of the spectral distributions of sun and comparison stars, we also observed a number of stars included in the absolute stellar calibration by Hayes (1970). The disadvantage of this calibration is that it applies only to regions which are free of spectral lines. To overcome this problem, we used Mihalas' (1966) hydrogen line-blanketed models. The star which was most suited for this purpose was HR 4468 (θ Crt, B9V), which is included in Hayes' calibration, has a spectral type covered by Mihalas' ($\log g, \theta$)-range, and is early enough to be considered still undisturbed by metal absorptions at the resolution of our photometric system.

A first direct comparison between our photometric system and Hayes' calibration, in which the energy distributions relative to HR 4468 are taken, showed both systems to be consistent within 2 percent in regions free of lines. The spectral range covered by this comparison was from B3V to A1V. Shortward of 0.36μ the deviations were somewhat larger for B3V but still did not exceed 5 percent.

The stellar model chosen for HR 4468 is specified by Mihalas with the parameters $\log g=4$, $\theta=0.45$. To convert the model into our photometric system, the filter bandpasses were assumed to be square.

With the information from the model it is possible to construct an energy distribution for each

Table I
Normalized Relative Reflectivities of Galilean Satellites

$\lambda(\mu)$	Io	Europa	Ganymede	Callisto
0.300	0.216	0.332	0.476	0.392
0.308	0.108	0.408	0.389	0.436
0.318	0.075	0.370	0.375	0.382
0.328	0.096	0.378	0.386	0.403
0.340	0.096	0.410	0.446	0.440
0.350	0.097	0.422	0.490	0.483
0.358	0.104	0.448	0.547	0.515
0.368	0.132	0.491	0.582	0.547
0.378	0.123	0.510	0.591	0.552
0.390	0.164	0.570	0.639	0.612
0.399	0.213	0.592	0.683	0.639
0.423	0.331	0.673	0.723	0.683
0.444	0.462	0.751	0.785	0.756
0.457	0.566	0.810	0.833	0.783
0.478	0.671	0.857	0.870	0.823
0.498	0.749	0.891	0.905	0.858
0.518	0.776	0.895	0.919	0.885
0.538	0.794	0.898	0.920	0.906
0.560	0.801	0.920	0.942	0.934
0.578	0.813	0.937	0.945	0.951
0.599	0.847	0.964	0.969	0.975
0.615	0.877	0.968	0.995	0.991
0.637	0.954	0.983	0.993	0.996
0.652	0.954	0.994	1.000	0.986
0.672	0.983	1.000	0.997	0.998
0.698	1.000	0.998	0.985	0.989
0.717	0.994	0.994	0.978	0.986
0.746	0.986	0.986	0.987	1.000
0.767	0.979	0.996	0.967	0.984
0.787	0.963	0.975	0.960	0.981
0.808	0.960	0.988	0.966	0.988
0.838	0.925	0.960	0.931	0.962
0.862	0.948	0.992	0.950	0.985
0.894	0.933	0.976	0.912	0.958
0.923	0.911	0.998	0.910	0.951
0.950	0.921	0.982	0.894	0.960
0.996	0.887	0.956	0.864	0.931
1.032	0.868	0.910	0.830	0.934
1.080	0.831	0.874	0.823	0.916
1.105	0.805	0.860	0.800	0.883

observed star. The energy distributions thus derived for a B3V star and an A1V (resp. HR 3454 and HR 4963) are from 0.45μ to 0.70μ , similar to Hayes' calibration for the regions where the influence of the hydrogen lines is negligible. Over this region the deviations do not exceed 2 percent. Shortward of 0.36μ the deviations were larger, if the energy distributions were matched over the range from 0.45μ to 0.70μ . This, however, can easily be caused by a slight mismatch of the model parameters. This seems to be the case, because the deviations are of the same order of magnitude and sign both for the A1V star and the B3V star. Since the deviations in this case were somewhat larger than the deviations between our system and Hayes' as mentioned before, at $\lambda < 0.36\mu$ we applied a correction for this.

The corrections, which are listed in Table II, are such that the energy distribution derived by the model has to be multiplied by the correction factor to be consistent with Hayes' calibrations.

TABLE II
Correction Factors Applied to Model-Derived Energy Distribution

λ (μ)	CORRECTION FACTOR
0.300	0.88
0.308	0.88
0.318	0.88
0.328	1.00
0.340	1.05
0.350	1.50

The two shortest wavelengths listed in Table II were assumed to need the same correction factor as determined for $\lambda=0.318\mu$; this may not be strictly correct in view of the trend longward of 0.318μ . At the long wavelength end of the spectrum there still remains the Paschen jump and the Paschen lines. However, the filter transmission bands are wider

in that region ($\Delta\lambda\sim 0.03\mu$). The Paschen jump, which is not very large, will tend to be smoothed out by the bandwidth and the effect of overlapping lines. For these reasons, we smoothed the energy distribution of the stellar model ($\log g = 4, \theta = 0.45$) through towards the longer wavelengths.

Figure 1 shows the energy distribution of HR 4030 (35 Leo) thus derived, from Mihalas' model ($\log g = 4, \theta = 0.45$) and the observations of HR 4030 and HR 4468. The dotted line is the energy distribution of the sun from Labs and Neckel (1968). Although in detail there are some discrepancies, the overall agreement is very good. At the two shortest wavelengths HR 4030 seems too high, but that could be caused by the fact that the correction factor derived for 0.318 was used. The match for the other solar-type stars observed was considerably worse. These will be discussed elsewhere.

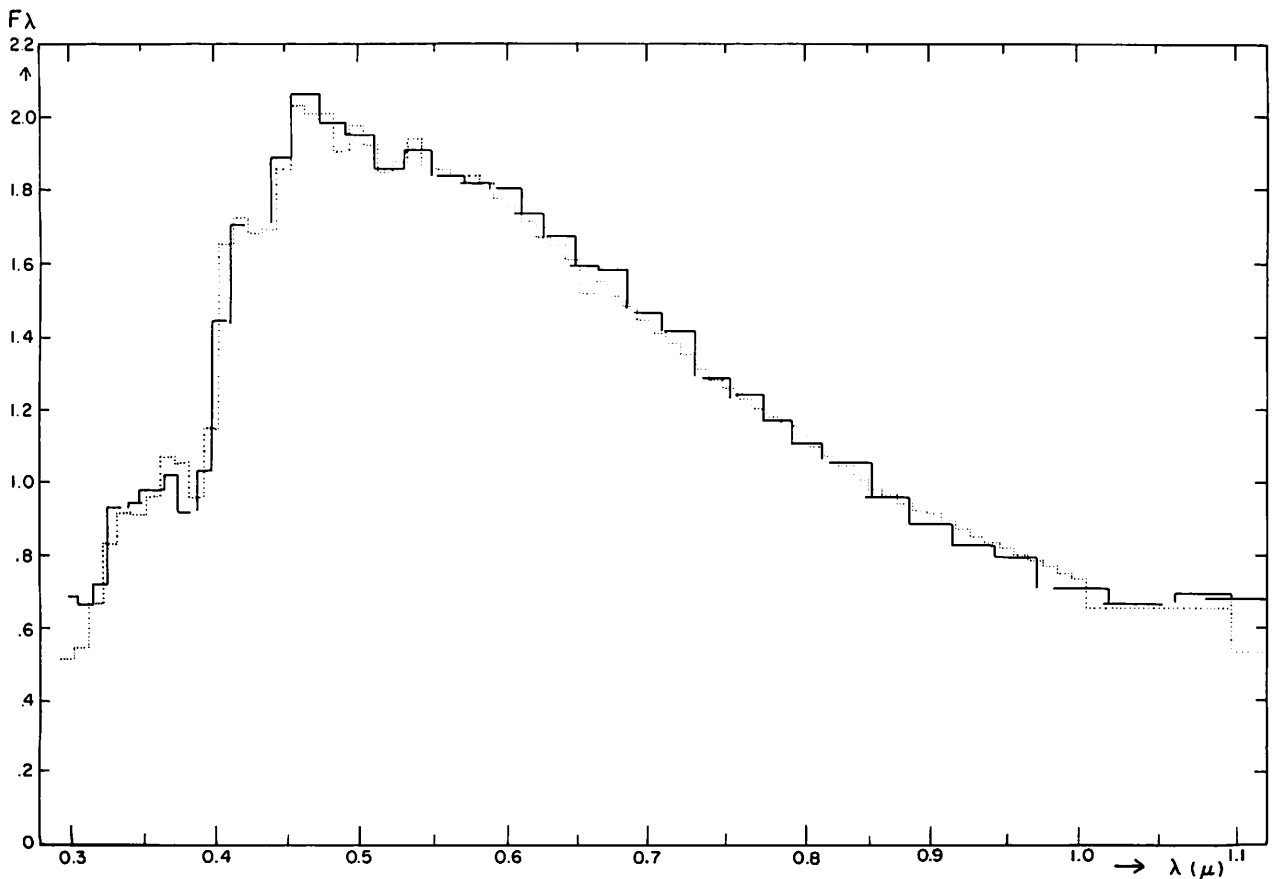


Fig. 1. Comparison between flux distributions of the sun (dotted line: Labs and Neckel 1968) and 35 Leo (HR 4030). Unit of F_λ is $\text{Wcm}^{-2}\mu^{-1} \times \text{const.}$

3. The Albedo Curves

Figure 2 shows the albedo wavelength curves for the Galilean satellites. The left-and-right hand ordinates are respectively normalized and geometrical albedos. The geometrical albedos used here are described in Appendix I. The error bars drawn in Figure 2 are the average deviations from the mean.

The normalized reflection curves for all four satellites look similar. They all show a decrease in the albedo towards shorter wavelengths. For Io the decrease starts around 0.7μ and for the three outer ones at $\sim 0.6\mu$. From 0.6μ longward the albedo curves are more or less flat with a slight decrease at the longest wavelengths. Apart from a shallow absorption feature between 0.5μ and 0.6μ , the

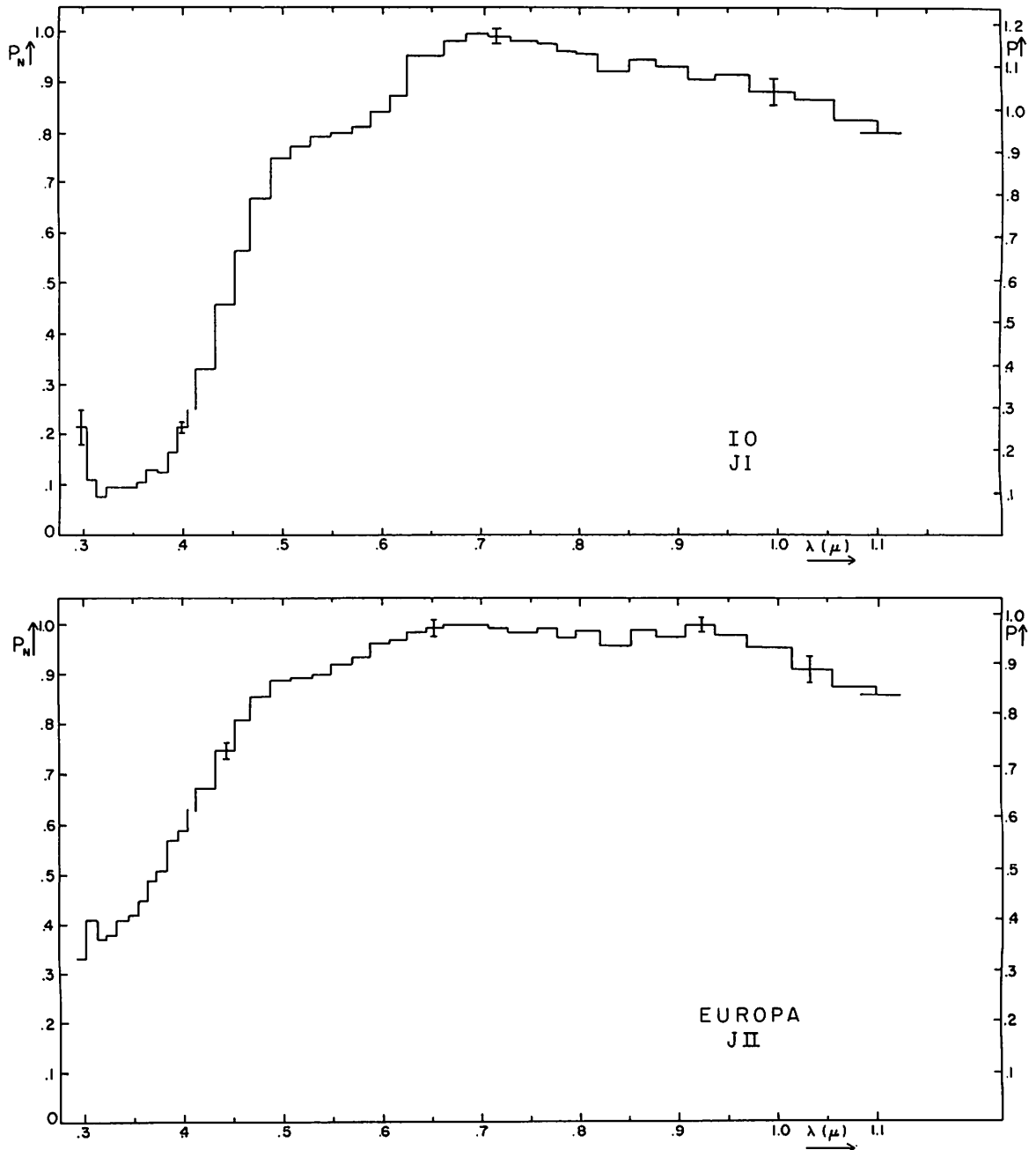


Fig. 2 Wavelength dependence of geometrical albedos of Galilean satellites; normalized albedos, P_n at left; geometrical albedos, P , derived in Appendix I, at right. Representative error bars show average deviations from the mean.

albedo curves are without any distinct features. This shallow feature is not present in the curve for J IV.

The curves are similar to the albedo-wavelength dependence found by Johnson (1971), but not identical. In the present data the absorption feature at $\lambda \sim 0.55\mu$ shown by Johnson for Io seems to be present also in the reflectivity curves for Europa and Ganymede, although less pronounced. Further,

Johnson's data show a stronger decrease in albedo longward of 0.95μ .

The similarity between the four satellites in the albedo-wavelength dependence exists only in the "normalized" curves. If one considers the geometrical albedos, a quite different picture emerges. In fact, the right-hand ordinates of Figure 2 show that the satellite albedos differ by a factor of 4.

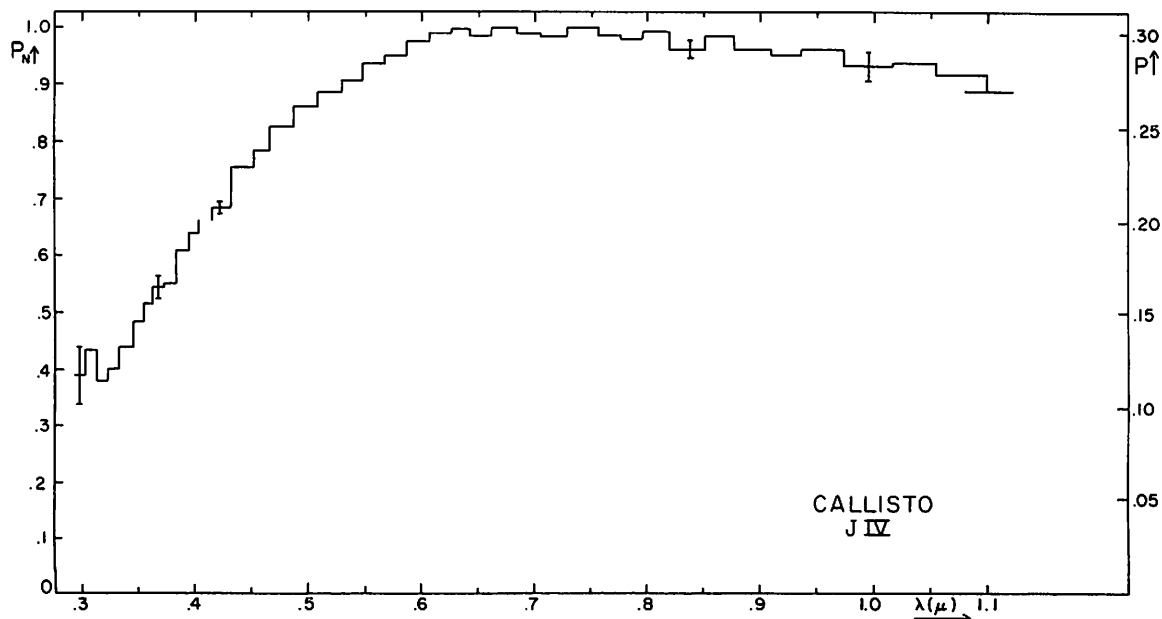
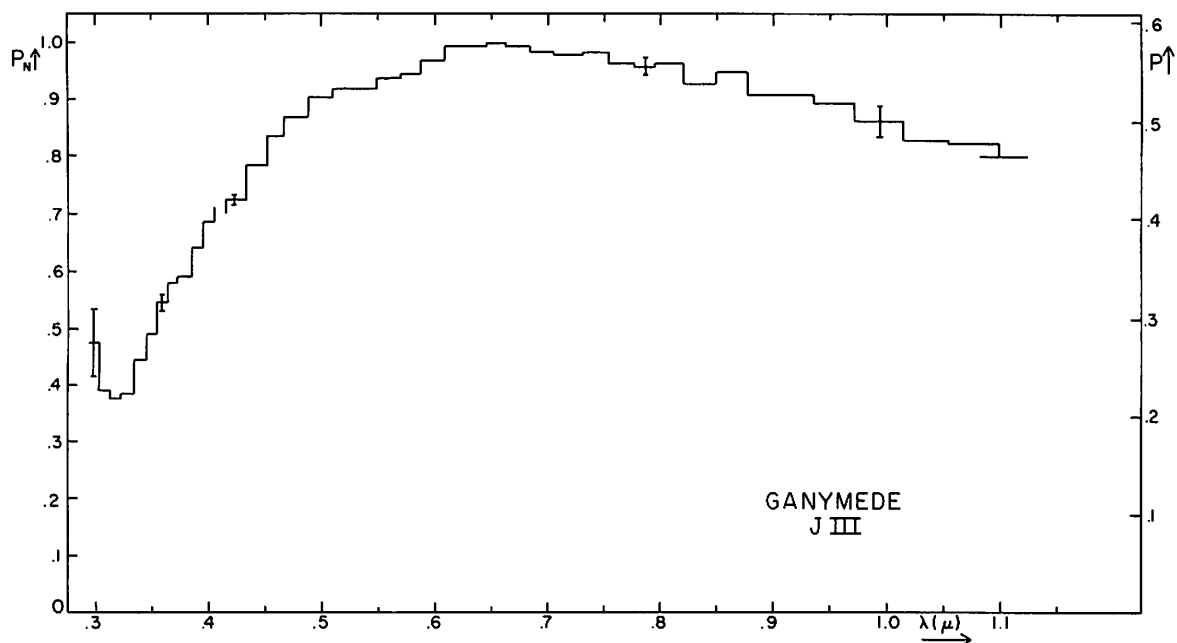


Fig. 2, continued.

Table III gives the highest and lowest albedos measured for each satellite, together with the wavelengths at which they occur.

TABLE III
Maximum and Minimum Albedos of Galilean Satellites
($0.3\mu < \lambda < 1.1\mu$)

	λ MAX	P MAX	λ MIN	P MIN
J I	0.70	1.18	0.32	0.09
J II	0.67	0.98	0.30	0.32
J III	0.65	0.58	0.32	0.22
J IV	0.75	0.30	0.32	0.12

Table III further indicates that, although the "normalized" albedo curves are similar in appearance, this does not imply similar surface materials, unless one assumes for each satellite an appropriate amount of a featureless greying agent. The high geometrical albedos make this assumption dubious. Also, the broad-band infrared data of Lee (1972) show dissimilarities between the satellites. The absence of distinct absorption features between 0.5μ and 1.1μ suggests the following possibilities (Adams 1968):

- (a) The absence of iron-bearing minerals.
- (b) Very small particles ($< 10\mu$) which reduce absorption because of reduced penetration.
- (c) The presence of substantial amounts of a highly absorbing material.

In view of the high albedos for JI, JII and JIII possibility (c) is improbable for them. The weakening of the absorptions by very small particles might be present. The absence of iron-bearing minerals seems confirmed. The most conspicuous common spectral feature of the satellites is the nearly uniform drop in reflectivity from $0.5-0.3\mu$. This has not been explained. Sulfur and some of its compounds exhibit this property, but its common presence on other solar-system bodies (the Moon, Mercury, Saturn's Rings) suggest other possibilities, such as radiation damage.

In the following we will see what additional conclusions can be drawn from the albedo wavelength dependence from 0.3μ to 1.1μ . We will also make use of the broad-band infrared data in the Johnson JHKL-system (Lee, *op. cit.*)

4. Io

The strong UV absorption appears to rule out a cover by ice. Although various substances studied by Sill (Sill 1972 and Kuiper 1969) show UV absorptions, most of these are not very strong. Of the more abundant substances only sulfur and some of its compounds match the general run of the Io

albedo curve. While some other compounds also show fairly strong UV absorptions, they are less probable on grounds of abundance. Now the slope of the UV sulfur absorption is dependent on the specific compounds; and, as is shown by Sill (1972), the position and slope of the ultraviolet absorption are temperature-dependent. The reflectivity of sulfur compounds increases with decreasing temperature, which might explain the high albedo of Io. Sill's reflection curves of ammonia compounds show a number of absorptions which are not seen in the albedo-wavelength dependence of Io. $\text{NH}_4 \cdot \text{HS}$ gives rise to absorptions centered at $\sim 0.6\mu$, $\sim 1.4\mu$, $\sim 1.7\mu$ and $\sim 2.3\mu$. The narrow-band data do show an absorption at $\sim 0.55\mu$ close to the 0.6μ absorption. However, the absorptions at $\lambda > 1.1\mu$ are of such strength and position that they would give rise to noticeable decrease in the observed albedo even in the broad-band data. The IR data of Lee do not show any depression. Thus there is no evidence for the presence of $\text{NH}_4 \cdot \text{HS}$, but S may be present.

5. Europa

The maximum albedo of JII is somewhat lower than that of Io, but still high. However, the UV absorption is considerably less strong. An absorption around 0.5μ seems to be present but is not very strong. The strength of the UV absorption of Europa is such that there exists a large range of compositional possibilities. Although the ferrous ion in most samples studied by Sill shows a UV absorption of the same order of magnitude as JII, most ferrous compounds show a low albedo. However, there exists observational evidence that Europa has polar caps (Veverka 1970). The region $\lambda > 1\mu$ must be consulted for additional clues. Lee's IR data suggest a close similarity between JII and JIII.

6. Ganymede and Callisto

The normalized albedos of these two satellites are very similar from 0.32μ to 0.92μ . With the observations having an accuracy of 2 percent, the ratio $p(\text{JIII})/p(\text{JIV})$ is found constant within the expected error limits.

However, both the absolute visual and the IR albedos are considerably different. Lee finds that the IR albedo of JIII is compatible with H_2O ice. If one makes a detailed comparison between the reflection spectrum of H_2O ice at -190°C (Kuiper *et al.*), the agreement is very good. The probable presence of H_2O on Europa and Ganymede was discovered by Kuiper (1957).

Acknowledgments. The work here reported was supported by NASA Grant No. NGL-03-002-002.

APPENDIX I

The Geometrical Albedo of The Galilean Satellites

Table IV lists the values of the geometrical albedos of the Jovian satellites at $\lambda_{\text{eff.}} = 0.55\mu$, as derived from both narrow- and broad-band observations. For the M_V of the sun we used Johnson's (1965) value of -27.64 . The radii used are from Kuiper (1952). A change in radius of ΔR will change the albedo with a factor $(1 + \Delta R/R)^2$. It is obvious from Table IV that the observational accuracy is fairly high. The main uncertainty in these numbers is still caused by the difficulty in measuring the diameter of the satellites. In determining the average value of the albedos, the measurement of Io by Lee is not taken into account. For the three other satellites all four data sets are used. The relative accuracy of the observed geometrical albedo thus derived is 3 per cent (m.e.).

TABLE IV

Geometric Albedos of the Galilean Satellites at $\lambda = 0.55 \mu$

	1) RADIUS (KM.)	2) HARRIS	3) LEE	4) JOHNSON	THIS PAPER	AVERAGE
Io	1625	0.97	(0.73)	0.91	0.94	0.94
Europa	1440	0.89	0.93	0.92	0.83	0.89
Ganymede	2510	0.52	0.51	0.57	0.54	0.54
Callisto	2230	0.27	0.27	0.30	0.27	0.28

1) Kuiper (1952); 2) Harris (1961); 3) Lee (1972); 4) Johnson and McCord (1970).

REFERENCES

- Adams, J. B. 1968, *Science*, **159**, 1453.
 Code, A. D. 1960, *Stars and Stellar Systems*, Vol. VI, ed. J. L. Greenstein (Chicago: University of Chicago Press), p. 50.
 Duke, M. B., Woo, C. C., Bird, M. L., Sellen, G. A., Finkelman, R. B. 1970, *Science*, **167**, 648.
 Harris, D. L. 1961, *Planets and Satellites*, eds. G. P. Kuiper and B. M. Middlehurst (Chicago: University of Chicago Press), p. 272.
 Hayes, D. S. 1970, *Ap. J.*, **159**, 165.
 Johnson, H. L., Mitchell, R. I. 1962, *LPL Comm. No. 14*, 1, 73.
 Johnson, H. L. 1965, *LPL Comm. No. 53*, 3, 73.
 Johnson, T. V., McCord, T. B. 1970, *Icarus*, **13**, 37.
 Johnson, T. V. 1971, *Icarus*, **14**, 94.
 Kuiper, G. P. 1952, *The Atmospheres of the Earth and Planets*, ed. G. P. Kuiper (Chicago: University of Chicago Press), p. 306.
 Kuiper, G. P. 1957, *Astron. J.*, **62**, 245.
 Kuiper, G. P. 1969, *LPL Comm. No. 101*, 6, 229.
 Kuiper, G. P., Cruikshank, D. P., Fink, U. 1970, *Sky and Telescope*, **39**, 80.
 Labs, D., Neckel H. 1968, *Zeitschrift für Astrophys.*, **69**, 1.
 Lee, T. A. 1972, *LPL Comm. No. 168*, 9, in press.
 McCord, T. B., Adams, T. B., Johnson, T. V. 1970, *Science*, **168**, 1445.
 Mihalas, D. 1966, *Ap. J.*, Supplement Series, **13**, 1.
 Sill, G. 1972, "Laboratory Spectra of Selected Solids," *LPL Comm.*, in press.
 Veverka, J. F. 1970, "Photometric and Polarimetric Studies of Minor Planets and Satellites," Harvard Thesis.